A Volume Integral Formulation for Solving Eddy Current Problems on Polyhedral Meshes

Paolo Bettini[1,2], Mauro Passarotto[3], and Ruben Specogna[3]

[1]Department of Industrial Engineering, University of Padova, 35131 Padua, Italy
[2]Consorzio RFX, 35127 Padova, Italy
[3]Polytechnic Department of Engineering and Architecture, Università di Udine, 33100 Udine, Italy

This paper presents a volume integral formulation to solve eddy current problems on general polyhedral meshes. The required topological preprocessing is efficiently addressed in linear worst case complexity by using the idea of lazy cohomology generators.

***Index Terms*— Cohomology, eddy currents, lazy generators polyhedral meshes, volume-integral (VI) formulation.**

I. Introduction

INTEGRAL formulations to solve eddy current problems, based on edge/face elements for tetrahedral and hexahedral meshes, have been developed a long time ago [1] and still are topical.

Yet, in the past few years, the interest in discretization methods for general polyhedral meshes has considerably grown. Polyhedral meshes, in fact, have the potential to allow faster and robust mesh generation and to enable novel techniques for adaptive mesh refinement, derefinement, and nonoverlapping domain decomposition with nonmatching grids. In particular, the nonconforming-like refinement—as the subgridding proposed in [4]—and the adaptive coarsening strategy [6] are particularly appealing.

This paper introduces for the first time an integral formulation for eddy current problems based on the discrete geometric approach [3] to solve eddy current problems on general polyhedral meshes. This formulation is based on the construction of the resistance **R** and magnetic **M** matrix with the face vector basis functions introduced in [4] and [5] that fulfill all desirable properties of consistency, symmetry, and positive definiteness that yield to stability.

The novel integral formulation is also able to treat manifold conductors $\mathcal{K}$ with arbitrary topology. To achieve good overall performances, it is mandatory to perform the required topological preprocessing efficiently; otherwise, this step easily becomes the bottleneck of the entire simulation. In this paper, we introduce for the first time the use of *lazy first cohomology group generators* $H^1(\partial\mathcal{K}, \mathbb{Z})$ of the boundary $\partial\mathcal{K}$ of the conductors [7]–[9] inside volumetric eddy current integral formulations. To present this part, we have necessarily used concepts of algebraic topology that due to the limited space cannot be recalled here. Please consult [10] for a formal introduction or [7] or [11] for an informal one.

This paper is organized as follows. In Section II, we introduce the novel formulation for polyhedral meshes.

Manuscript received November 19, 2016; accepted January 27, 2017. Date of publication February 2, 2017; date of current version May 26, 2017. Corresponding author: P. Bettini (e-mail: paolo.bettini@unipd.it).

Color versions of one or more of the figures in this paper are available online at http://ieeexplore.ieee.org.

Digital Object Identifier 10.1109/TMAG.2017.2663112

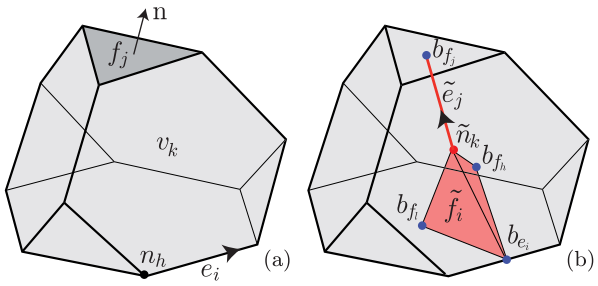

Fig. 1. (a) Edge e_i and a face f_j of a polyhedron v_k in $\mathcal{K}$. (b) Dual face $\tilde{f}_i = D(e_i)$ dual to edge e_i and dual edge $\tilde{e}_j = D(f_j)$ dual to face f_j.

Section III addresses the topological preprocessing required to obtain a well-posed problem when the domain is topologically nontrivial. Section IV deals with the computation of the resistance **R** and magnetic **M** matrices. In Section V, we validate the formulation in three test cases. Finally, in Section VI, conclusions are drawn.

II. Integral Formulation for Polyhedral Meshes

Let us consider the geometric elements of a polyhedron v_k shown in Fig. 1 belonging to the mesh representing the conductors of the eddy current problem made of N_v polyhedral elements. We denote with e_i a generic-oriented edge and with f_j an oriented face, where $i = 1, \ldots, N_e^k$, $j = 1, \ldots, N_f^k$, N_e^k, with N_f^k being the number of edges and faces of v_k, respectively. In Fig. 1, the oriented dual edge $\tilde{e}_j = D(f_j)$ and the oriented dual face $\tilde{f}_i = D(e_i)$ of an interlocked dual mesh are additionally shown, where D is the duality operator. Such a dual mesh is produced with barycentric subdivision since the barycenters b_{e_i} and b_{f_j} of e_i and of f_j are needed, respectively, for its construction. Finally, the dual node $\tilde{n}_k = D(v_k)$ has an arbitrary location in v_k. Vector e_i, denoted in roman type, is the edge vector associated with e_i, whereas vector f_j is the face vector associated with the face f_j defined as $\mathrm{f}_j = \int_{f_j} \mathrm{n} ds$, where n is the unit vector normal to and oriented as f_j. Similarly, vector $\tilde{\mathrm{f}}_i$ is the face vector associated with the face $\tilde{f}_i$ and $\tilde{\mathrm{e}}_j$ is the edge vector associated with the edge $\tilde{e}_j$. By construction, $\mathrm{e}_i \cdot \tilde{\mathrm{f}}_i > 0$ and $\mathrm{f}_j \cdot \tilde{\mathrm{e}}_j > 0$ hold. The volume V_k of v_k can be equivalently computed [4] as $V_k = \frac{1}{3}\sum_{i=1}^{N_f^k} \mathrm{f}_i \cdot \tilde{\mathrm{e}}_i = \frac{1}{3}\sum_{i=1}^{N_e^k} \mathrm{e}_i \cdot \tilde{\mathrm{f}}_i$.

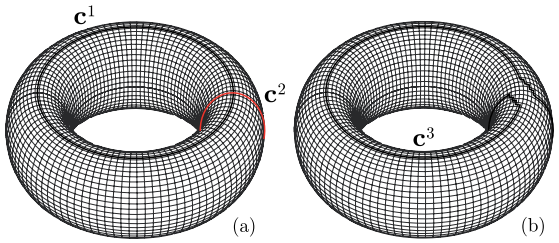

Fig. 2. (a) Dual in $\partial\mathcal{K}$ of the support of the 1-cocycle $\mathbf{c}^1$, which is bounding in the complement of $\mathcal{K}$, and $\mathbf{c}^2$, which is bounding inside $\mathcal{K}$. (b) Support of the dual in $\partial\mathcal{K}$ of a "mixed" generator nontrivial in $H^1(\partial\mathcal{K}, \mathbb{Z})$.

We define the degrees of freedom (DOFs) to be the circulations of the electric vector potential on mesh edges. Let us introduce the vector collecting all of them as $\mathbf{T}$. Then, we introduce the array containing the electric currents on faces of the mesh through $\mathbf{I} = \mathbf{C}(\mathbf{T} + \mathbf{Hi})$, where $\mathbf{C}$ is the incidence matrix between face and edge pairs, $\mathbf{i}$ is the array with the unknown *independent currents* [9], and $\mathbf{H}$ stores a set of representatives of the first cohomology group generators $H^1(\partial\mathcal{K}, \mathbb{Z})$ of the boundary $\partial\mathcal{K}$ of the conductors. The potentials are such that the discrete current continuity law holds ($\mathbf{DI} = \mathbf{0}$), where $\mathbf{D}$ is the incidence matrix between volume and face pairs.

The system equations are obtained by enforcing the discrete Faraday law $\mathbf{C}^T\tilde{\mathbf{U}} + i\omega\tilde{\mathbf{\Phi}} = \mathbf{0}$, where $\tilde{\mathbf{U}}$ represents the array of electromotive forces on dual edges whereas $\tilde{\mathbf{\Phi}}$ is the magnetic flux on dual faces. By definition, $\tilde{\mathbf{\Phi}} = \mathbf{C}^T(\mathbf{A} + \mathbf{A}_s)$, where $\mathbf{A}$ and $\mathbf{A}_s$ are the circulations of the magnetic vector potential on dual edges due to eddy currents and source currents, respectively. By recalling that $\tilde{\mathbf{U}} = \mathbf{RI}$ and $\tilde{\mathbf{A}} = \mathbf{MI}$, we define $\mathbf{K} = \mathbf{C}^T(\mathbf{R} + i\omega\mathbf{M})\mathbf{C}$ and finally get

$$\mathbf{KT} + (\mathbf{KH})\mathbf{i} = -i\omega\mathbf{C}^T\tilde{\mathbf{A}}_s, \tag{1}$$

$$(\mathbf{H}^T\mathbf{K})\mathbf{T} + (\mathbf{H}^T\mathbf{KH})\mathbf{i} = -i\omega\mathbf{H}^T\mathbf{C}^T\tilde{\mathbf{A}}_s. \tag{2}$$

Finally, we apply boundary conditions by setting to zero the DOFs on $\partial\mathcal{K}$. To reduce the unknowns, we apply the standard tree-cotree gauge [1] by setting again the DOFs to be zero on a suitable tree inside $\mathcal{K}$.

III. Efficient Topological Preprocessing

The topological preprocessing for integral formulations is expected to find a maximal set of boundary 1-cocycles that are independent in the first cohomology group $H^1(\partial\mathcal{K}, \mathbb{Z})$ and their dual in $\partial\mathcal{K}$ are bounding with respect to the exterior of $\mathcal{K}$ [12].

To clarify this point, let us consider as a conductor $\mathcal{K}$ the solid torus represented in Fig. 2(a). A possible basis for $H^1(\partial\mathcal{K}, \mathbb{Z})$ is obtained by taking the two representatives $\mathbf{c}^1$ and $\mathbf{c}^2$ of generators whose dual of their support in $\partial\mathcal{K}$ is represented in Fig. 2(a). The dual of $\mathbf{c}^1$ in $\partial\mathcal{K}$ is bounding in the complement of $\mathcal{K}$ and, therefore, this cocycle is topologically interesting. On the contrary, $\mathbf{c}^2$ is not interesting given that the dual 1-cycle $D(\mathbf{C}\,\mathbf{c}^2)$ is bounding inside $\mathcal{K}$ and so nonlocal Faraday's laws on it is a linear combination of (1).

Disentangling boundary generators is far from being trivial, because it is, in general, not enough to pick half of the generators to produce the suitable basis. The boundary generators, in fact, may be "mixed" (i.e., a linear combination of $\mathbf{c}^1$ and $\mathbf{c}^2$) as $\mathbf{c}^3$ in Fig. 2(c). Thus, there are no easier ways to solve the problem than the change of basis described in [12], a step that has been always deemed as necessary [12], [13].

In this paper, we propose a different solution based on using the *lazy cohomology generators* [7]–[9] inside integral formulations. The recipe is to use all boundary $H^1(\partial\mathcal{K}, \mathbb{Z})$ generators that indeed span the suitable cohomology group even if they are not linearly independent.

This technique is appealing first of all because the topological preprocessing requires mere seconds even on very complicated examples due to the fact that they can be obtained in linear worst case complexity with the algorithm described in [9]. Moreover, the algorithm is easy to code since it is combinatorial and it does not require any arithmetics on integers. Despite all of these advantages, the obtained solution in terms of induced currents obtained with lazy generators is the same, up to linear solver tolerance, with the one employing standard cohomology generators. Moreover, there is no degradation of performances in the linear solver when using lazy generators in place of standard ones.

IV. Computation of $\mathbf{R}$ and $\mathbf{M}$ Matrices

A. Face Piecewise-Uniform Basis Functions in v_k

Let us define T_i as $T_i = \tilde{e}_i \otimes f_i, \forall i = 1, ..., N_f^k$, where $\tilde{e}_i = D(f_i)$ and $\otimes$ is the Kronecker product. The trace $t_i = tr(T_i)$ of T is thus $t_i = tr(T_i) = \tilde{e}_i \cdot f_i, \forall i = 1, ..., N_f^k$. Assuming the current density $\mathrm{j}(p)$ uniform in v_k, we reconstruct it as

$$\mathrm{j}(p) = \sum_{i=1}^{N_f^k} w_i^k(p)\mathbf{I}_{f_i}^k \tag{3}$$

where $p \in v_k$, $\mathbf{I}_{f_i}^k$ is the current on the ith face of v_k

$$\mathbf{I}_{f_i}^k = \int_{f_i} \mathrm{j}(p) \cdot \mathrm{n}\, ds \tag{4}$$

and $w_i^k(p)$ are the face basis vector functions defined in [4]

$$w_i^k(p) = \frac{\tilde{e}_j}{t_j}\delta_{ij} + \left(I_d - \frac{T_j}{t_j}\right)\frac{\tilde{e}_i}{V_k} \tag{5}$$

where I_d is the identity matrix, δ_{ij} is the Kronecker delta, and the basis function of the ith face of v_k is piecewise uniform in v_k and uniform in each τ_j^k for each $j = 1, ..., N_f^k$. τ_j^k is a pyramid having f_j as its base and $\tilde{n}_k$ as its apex.

B. Construction of $\mathbf{R}$

The i, j entry of the local resistance matrix for the element v_k of resistivity η is constructed as [4]

$$R_{ij}^k = \int_{v_k} w_i^k(p) \cdot \eta w_j^k(p)\, dv \quad i, j = 1, ..., N_f^k. \tag{6}$$

The integration is exact since the basis functions are piecewise uniform in τ_j^k regions. Let $p_h \in \tau_h^k$, then

$$R_{ij}^k = \sum_{h=1}^{N_f^k} w_i^k(p_h) \cdot \eta w_j^k(p_h)\frac{t_h}{3}. \tag{7}$$

TABLE I
SPHERE'S MESHES: NUMBER OF ELEMENTS (n_v), FACES(n_f), EDGES (n_e), NODES (n_n), AND DOFs

	n_v	n_f	n_e	n_n	DOF
mesh 1	1840	7256	7326	1911	4329
mesh 2	5912	21872	22014	6055	13505
mesh 3	13776	48860	49110	14027	30661

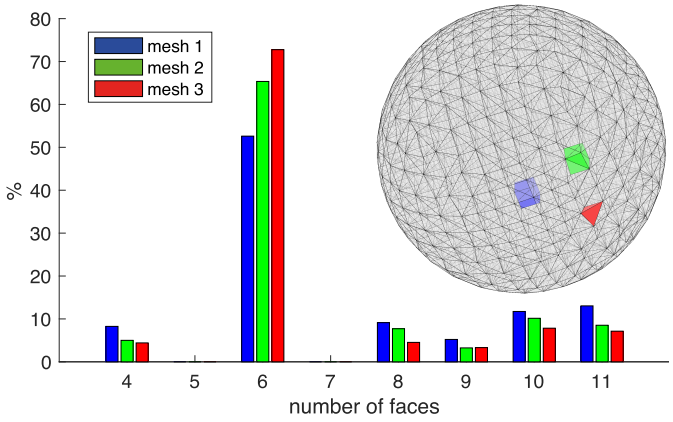

Fig. 3. Percentage of different kinds of polyhedra used in sphere's meshes 1 (coarse), 2 (intermediate), and 3 (fine). Inset: mesh 1: a tetrahedron (red), a hexahedron (blue), and a polyhedron with 11 faces (green) are shown.

C. Construction of **M**

The construction of matrix **M** starts from the Biot–Savart law that relates $\mathrm{j}(p)$ to the magnetic vector potential $\mathrm{a}(r)$, $r \in \mathcal{K}$

$$\mathrm{a}(r) = \frac{\mu}{4\pi} \int_{\mathcal{K}} \frac{\mathrm{j}(p)}{|r-p|}\, dv = \frac{\mu}{4\pi} \sum_{k=1}^{N_v} \int_{v_k} \frac{\mathrm{j}(p)}{|r-p|} dv. \quad (8)$$

Assuming again j as uniform inside v_k, we expand j with (3) getting

$$\mathrm{a}(r) = \frac{\mu}{4\pi} \sum_{k=1}^{N_v} \sum_{j=1}^{N_f^k} \mathbf{I}_{f_j}^k \int_{v_k} \frac{w_j^k(p)}{|r-p|} dv. \quad (9)$$

Let us now exploit the consistency property [4, Property 3] and note that if $\mathrm{a}(r)$, $r \in v_h$ is uniform inside v_h, we have

$$\tilde{\mathbf{A}}_{\tilde{e}_i}^h = \int_{\tilde{e}_i} \mathrm{a}(r) \cdot dl = \int_{v_h} \mathrm{a}(r) \cdot w_i^h(r)\, dv \quad (10)$$

where $\tilde{\mathbf{A}}_{\tilde{e}_i}^h$ is the circulation of $\mathrm{a}(r)$ on the part of the dual edge $\tilde{e}_i$ inside v_h. By substituting (9) inside (10), we get

$$\tilde{\mathbf{A}}_{\tilde{e}_i}^h = \frac{\mu}{4\pi} \sum_{k=1}^{N_v} \sum_{j=1}^{N_f^k} \mathbf{I}_{f_j}^k \int_{v_h} \int_{v_k} \frac{w_i^h(r) \cdot w_j^k(p)}{|r-p|}\, dv_r\, dv_p. \quad (11)$$

Therefore, the i, j entry of the local magnetic matrix between two given volumes v_h and v_k is

$$M_{ij}^{hk} = \frac{\mu}{4\pi} \int_{v_h} \int_{v_k} \frac{w_i^h(r) \cdot w_j^k(p)}{|r-p|}\, dv_r\, dv_p. \quad (12)$$

The magnetic vector potential $\mathrm{a}(r)$ and the magnetic flux density $\mathrm{b}(r)$ are computed by an efficient implementation on the GPU architecture [14] of the closed-form expressions introduced in [15], well suited for the adopted data structure.

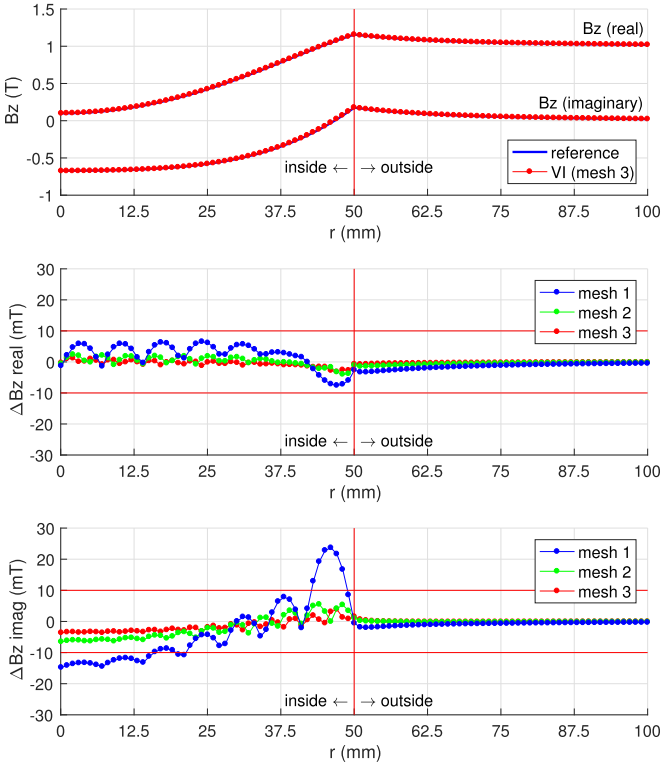

Fig. 4. Top: comparison of computed (VI) versus reference (analytical) solution in terms of B_z (real and imaginary components) along a radial path ($y = 0, z = 0$, $x \in [0, 100]$). Middle and bottom: ΔB_z real and imaginary components.

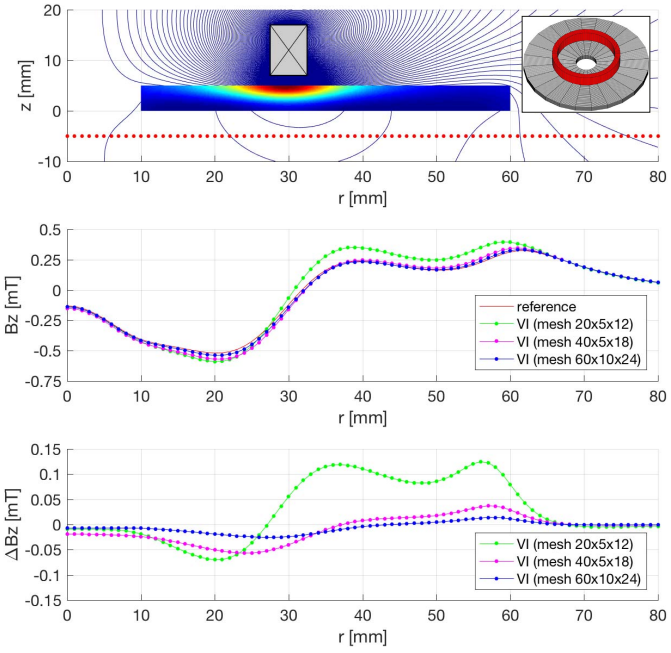

Fig. 5. Top: 2-D axisymmetric reference configuration (stranded coil, 1000 ampere-turns, $f = 1$ kHz, above a thick copper disk with one hole). Inset: 3-D mesh ($60 \times 10 \times 24$). Middle: VI versus reference. B_z (real component) along the radial path in the top figure (red dots) for three meshes. Bottom: $\Delta Bz = B_z^{VI} - B_z^{ref}$ (real component).

V. NUMERICAL RESULTS

Three test cases are considered to validate the implementation in the frequency domain.

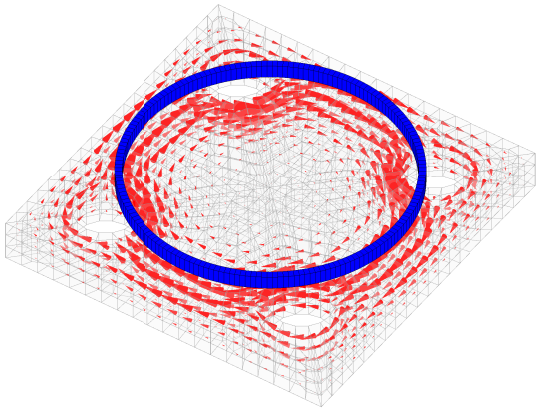

Fig. 6. Conducting domain is discretized in 1656 polyhedra, 5736 faces, 6567 faces, and 2484 nodes. The field source is an axisymmetric coil (blue) fed by an ac current at $f = 50$ Hz. Red cones: real part of J, not to scale.

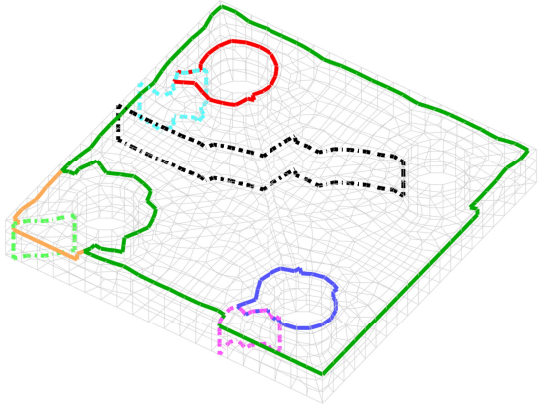

Fig. 7. Dual of the support in $\partial\mathcal{K}$ of four 1-cocycles nontrivial in $\mathcal{K}$ (solid lines) and four trivial (dashed lines).

1) A solid sphere (radius $a = 1$m, resistivity $\rho = 0.017\ \mu\Omega$m) in a uniform field (1T and $f = 50$ Hz).
2) A thick disk ($\rho = 0.017\ \mu\Omega$m) with one hole, excited by a stranded coil (1000 AT and $f = 1$ kHz).
3) A thick plate ($\rho = 0.017\ \mu\Omega$m) with four holes, excited by a stranded coil (1000 AT and $f = 50$ Hz).

In Fig. 4, the numerical results for three levels of discretization of the sphere used in test 1 (see Table I and Fig. 3) are compared to the analytical solution. Excellent agreement is found in all field points outside the sphere, for all meshes; inside the sphere, the discrepancy (ΔB_z) for mesh 1 is much higher than 2 and 3, as expected, given its coarseness.

The numerical solution of test 2 obtained with the *lazy cohomology basis* is the same as the one with the standard cohomology basis up to the linear solver tolerance. The numerical results for three levels of discretization are compared to the reference solution (2-D axisymmetric) in Fig. 5 fairly good agreement is found also with a relatively low number of elements (40×5 on the cross section with 18 subdivisions along the toroidal direction).

Finally, the results of test 3 are shown in Fig. 6. It is worth noticing that the solution obtained with the *lazy cohomology basis* (eight 1-cocycles, see the dual of their supports in Fig. 7) is again the same as the one obtained with the standard cohomology basis up to the linear solver tolerance and is in excellent agreement with the one computed by the 3-D FEM code computer-aided fusion engineering [16].

VI. Conclusion

A novel volume integral nonconforming formulation for solving eddy current problems in conductors of arbitrary topology discretized with general polyhedral meshes has been presented and validated against reference solutions.

Acknowledgment

This work was supported by the University of Padova under Grant CPDA144817.

The authors would like to thank the support of NVIDIA Corporation with the donation of the Tesla K40 GPU used for this research.

References

[1] R. Albanese and G. Rubinacci, "Integral formulation for 3D eddy-current computation using edge elements," *Proc. Inst. Elect. Eng. A, Phys. Sci., Meas. Instrum., Manage. Edu.-Rev.*, vol. 135, no. 7, pp. 457–462, Sep. 1988.

[2] J. Siau, G. Meunier, O. Chadebec, J.-M. Guichon, and R. Perrin-Bit, "Volume integral formulation using face elements for electromagnetic problem considering conductors and dielectrics," *IEEE Trans. Electromagn. Compat.*, vol. 58, no. 5, pp. 1587–1594, Oct. 2016.

[3] L. Codecasa, R. Specogna, and F. Trevisan, "A geometric integral formulation for eddy-currents," *Int. J. Numer. Meth. Eng.*, vol. 82, no. 13, pp. 1720–1736, 2010.

[4] L. Codecasa, R. Specogna, and F. Trevisan, "A new set of basis functions for the discrete geometric approach," *J. Comput. Phys.*, vol. 229, no. 19, pp. 7401–7410, 2010.

[5] L. Codecasa, R. Specogna, and F. Trevisan, "Geometrically defined basis functions for polyhedral elements with applications to computational electromagnetics," *ESAIM, M2AN*, vol. 50, no. 3, pp. 677–698, 2016.

[6] D. A. Di Pietro and R. Specogna, "An a posteriori-driven adaptive Mixed High-Order method with application to electrostatics," *J. Comput. Phys.*, vol. 326, pp. 35–55, Dec. 2016.

[7] P. Dłotko and R. Specogna, "Physics inspired algorithms for (co)homology computations of three-dimensional combinatorial manifolds with boundary," *Comput. Phys. Commun.*, vol. 184, no. 10, pp. 2257–2266, Oct. 2013.

[8] P. Dłotko and R. Specogna, "Lazy cohomology generators: A breakthrough in (co)homology computations for CEM," *IEEE Trans. Magn.*, vol. 50, no. 2, Feb. 2014, Art. no. 7014204.

[9] P. Bettini and R. Specogna, "Computation of stationary 3D halo currents in fusion devices with accuracy control," *J. Comput. Phys.*, vol. 273, pp. 100–117, Sep. 2014.

[10] J. R. Munkres, *Elements of Algebraic Topology*. Cambridge, MA, USA: Perseus Books, 1984.

[11] P. Dłotko and R. Specogna, "Cohomology in 3D magneto-quasistatics modeling," *Commun. Comput. Phys.*, vol. 14, no. 1, pp. 48–76, 2013.

[12] R. Hiptmair and J. Ostrowski, "Generators of $H_1(\Gamma_h, \mathbb{Z})$ for triangulated surfaces: Construction and classification," *SIAM J. Comput.*, vol. 31, no. 5, pp. 1405–1423, 2002.

[13] G. Rubinacci and A. Tamburrino, "Automatic treatment of multiply connected regions in integral formulations," *IEEE Trans. Magn.*, vol. 46, no. 8, pp. 2791–2794, Aug. 2010.

[14] T. Maceina, P. Bettini, G. Manduchi, and M. Passarotto, "Fast and efficient algorithms for computational electromagnetics on GPU architecture," presented at the 20th IEEE-NPSS Real Time Conf., Padua, Italy, Jun. 2016, pp. 6–10.

[15] M. Fabbri, "Magnetic flux density and vector potential of uniform polyhedral sources," *IEEE Trans. Magn.*, vol. 44, no. 1, pp. 32–36, Jan. 2008.

[16] P. Bettini, L. Marrelli, and R. Specogna, "Calculation of 3-D magnetic fields produced by MHD active control systems in fusion devices," *IEEE Trans. Magn.*, vol. 50, no. 2, Feb. 2014, Art. no. 7000904.